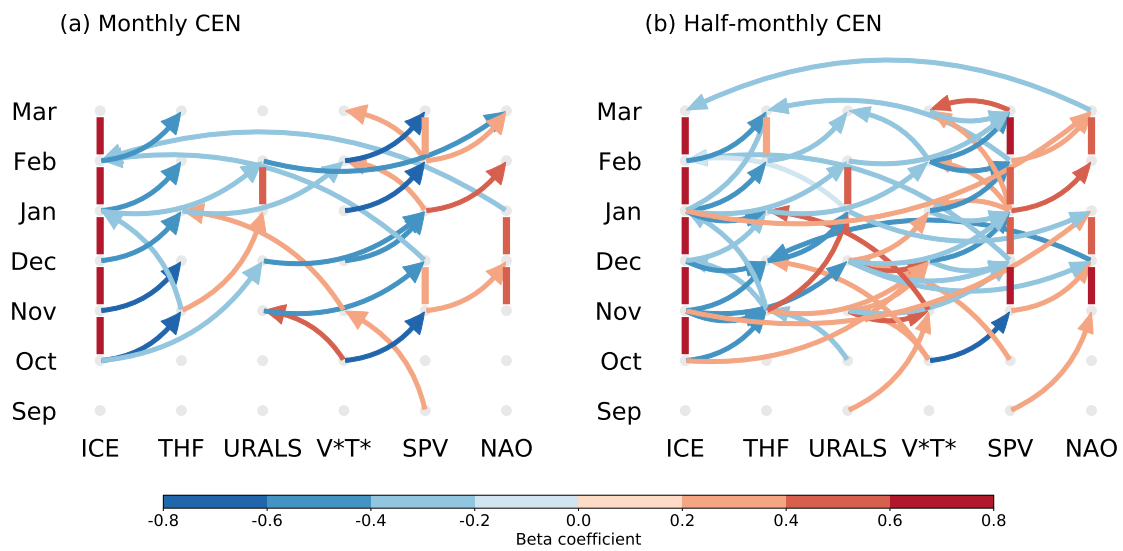
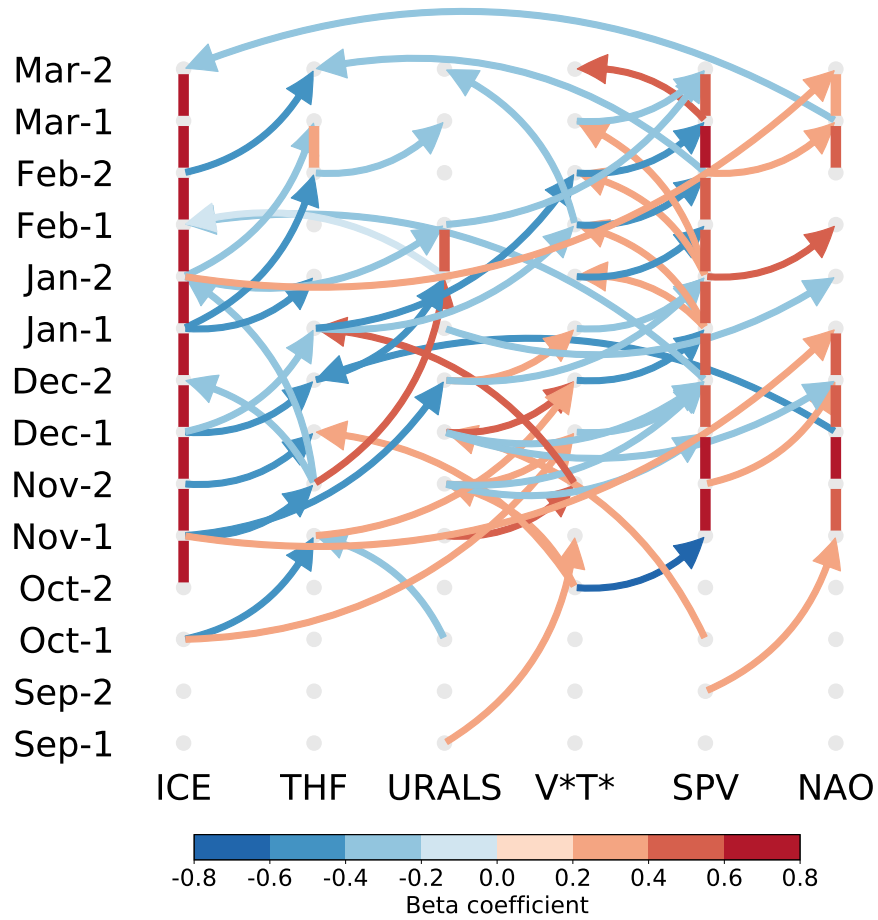


List of Figures

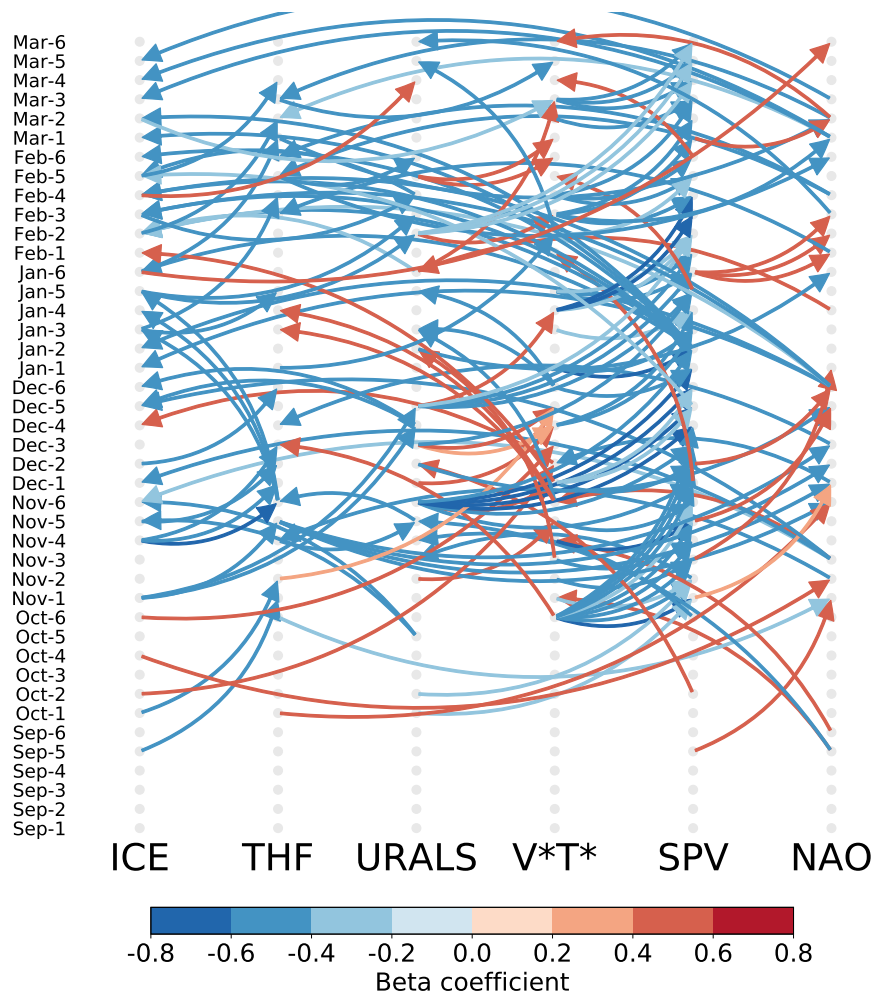
1	Same as Fig. 3, but showing the beta coefficients (colours) of all other casual linkages other than the stratospheric pathway. Note that the simultaneous relationship $\downarrow \text{URALS}_{Dec} \Rightarrow \uparrow \text{V}^*\text{T}^*_{Dec}$ (coloured horizontal line in Fig. 3a) is not shown here.	2
2	The unaggregated version of the half-monthly CEN. It forms Fig. S1b or Fig. 3b after aggregation.	3
3	Pentad average CEN with indices chosen as the monthly (Fig. 3a; fig. S1a) and half-monthly (Fig. 3b; fig. S1b) CENs. Linkages are at the 1% significance level. A maximum lag of 12 pentads (i.e., 2 months) is allowed. Autocorrelation is not used.	4
4	Additional detected causal linkages in the monthly CEN, following Kretschmer et al. 2016 that allows all other indices to be tested in the multiple regression equation (Eq. 4) along with the retained drivers. See section 2.2 for details.	5
5	Same as Fig. S1a, but additionally showing the occurrences rates of all linkages in the bootstrapped test. The occurrences rates of the stratospheric pathway and their distributions of beta coefficients are shown in Fig. 4.	6
6	Pentad average CEN using indices of download longwave radiation (IR), Barents-Kara sea ice (ICE) and Urals sea level pressure (URALS). A maximum lag of 2 pentads is allowed. Autocorrelation is not used. Fig. 7 is aggregated from this figure by by summing the number of times each linkage appears over the extended winter season.	7
7	Scatter plots between February NAO and late fall (mean of October and November) Barents-Kara sea ice in the period of 1979/80 to 2017/18. Shadings is DJF Nino3.4 index. Reds (blues) denote El Niño and La Niña events.	8
8	Same as Fig. S1a, but introducing index of downward longwave radiation (IR) into the monthly CEN.	9



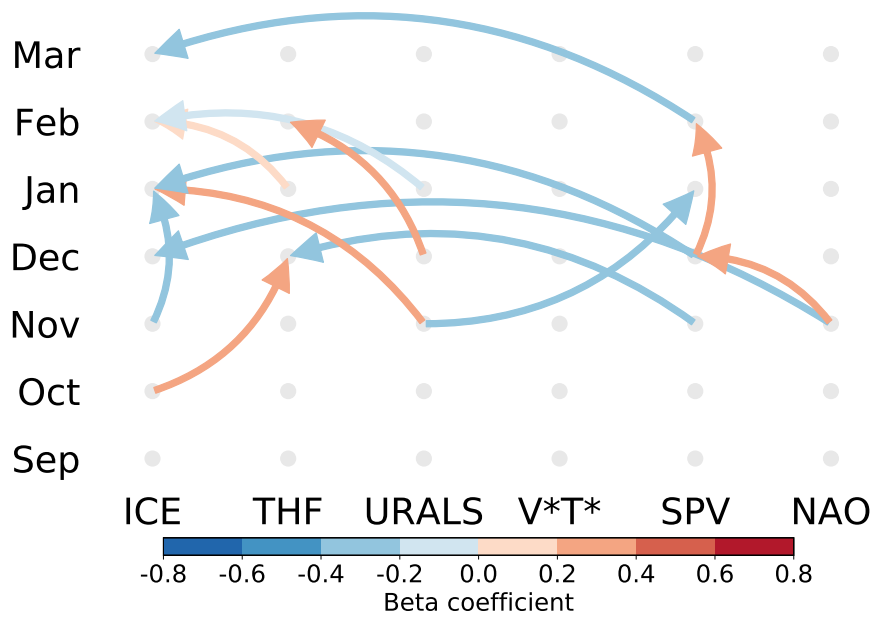
Supplementary Figure 1: Same as Fig. 3, but showing the beta coefficients (colours) of all other casual linkages other than the stratospheric pathway. Note that the simultaneous relationship $\downarrow \text{URALS}_{Dec} \Rightarrow \uparrow \text{V}^*\text{T}^*_{Dec}$ (coloured horizontal line in Fig. 3a) is not shown here.



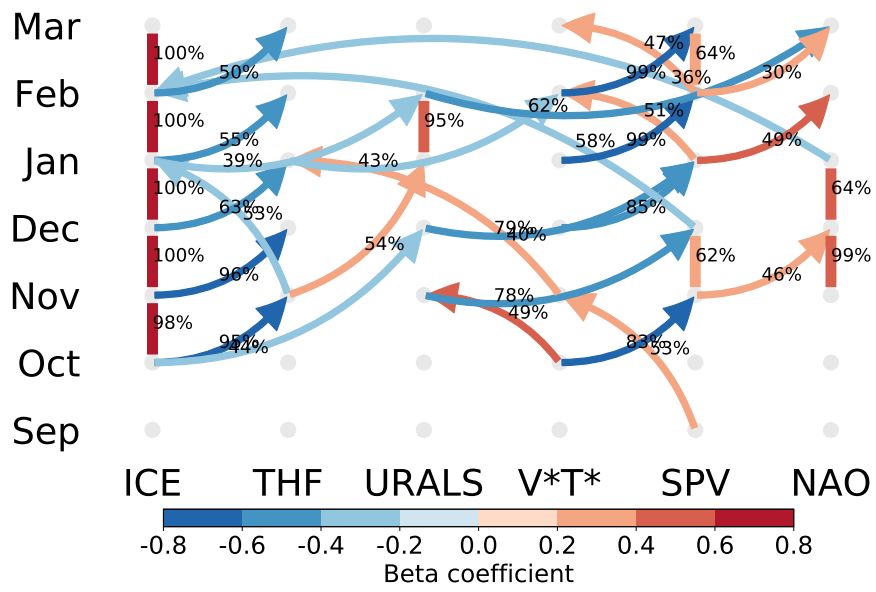
Supplementary Figure 2: The unaggregated version of the half-monthly CEN. It forms Fig. S1b or Fig. 3b after aggregation.



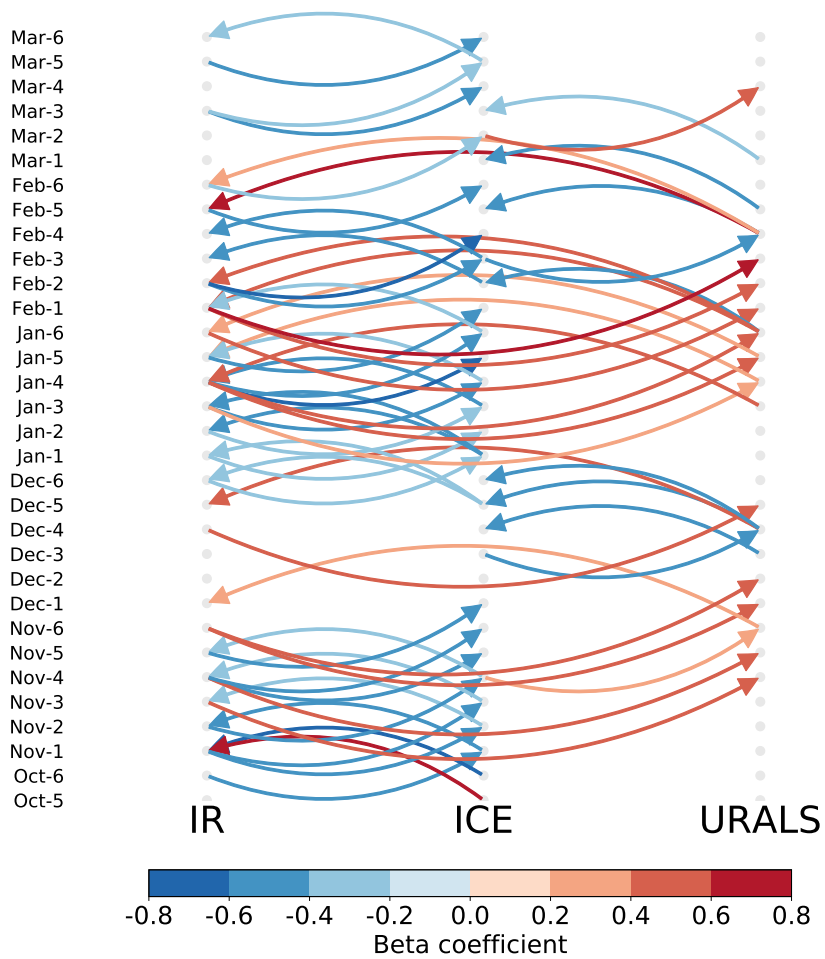
Supplementary Figure 3: Petnad average CEN with indices chosen as the monthly (Fig. 3a; fig. S1a) and half-monthly (Fig. 3b; fig. S1b) CENs. Linkages are at the 1% significance level. A maximum lag of 12 pentads (i.e., 2 months) is allowed. Autocorrelation is not used.



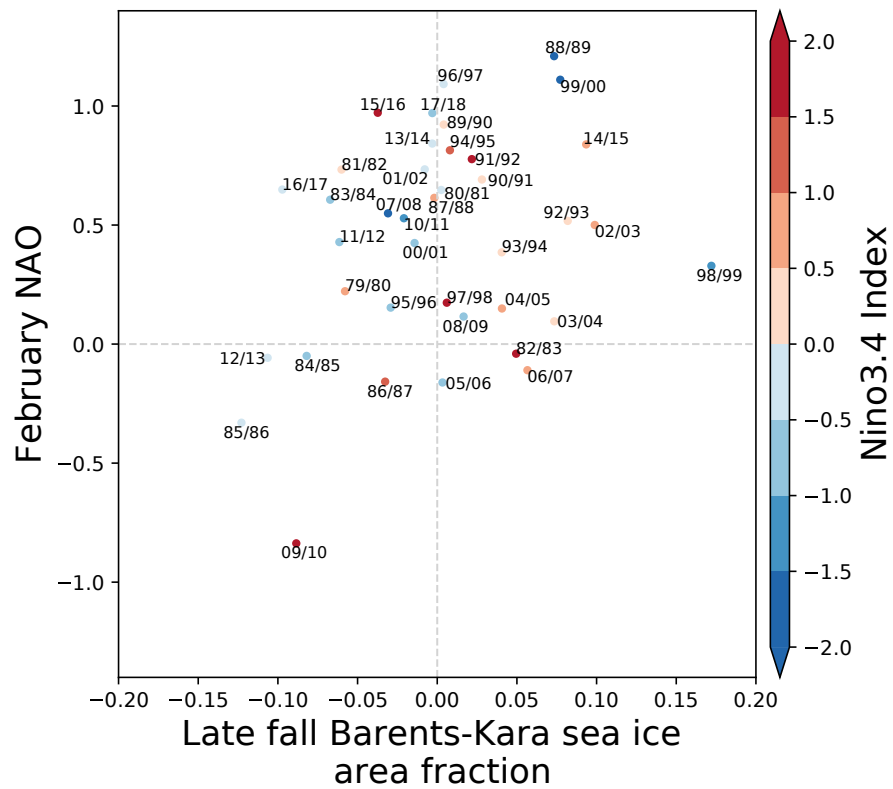
Supplementary Figure 4: Additional detected causal linkages in the monthly CEN, following Kretschmer et al. 2016 that allows all other indices to be tested in the multiple regression equation (Eq. 4) along with the retained drivers. See section 2.2 for details.



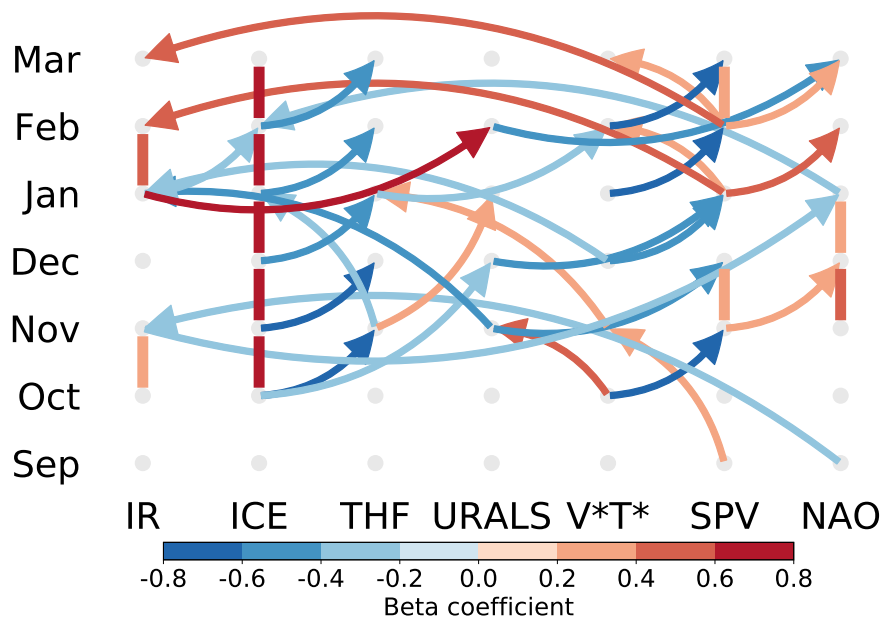
Supplementary Figure 5: Same as Fig. S1a, but additionally showing the occurrences rates of all linkages in the bootstrapped test. The occurrences rates of the stratospheric pathway and their distributions of beta coefficients are shown in Fig. 4.



Supplementary Figure 6: Pentad average CEN using indices of downwelling long-wave radiation (IR), Barents-Kara sea ice (ICE) and Urals sea level pressure (URALS). A maximum lag of 2 pentads is allowed. Autocorrelation is not used. Fig. 7 is aggregated from this figure by summing the number of times each linkage appears over the extended winter season.



Supplementary Figure 7: Scatter plots between February NAO and late fall (mean of October and November) Barents-Kara sea ice in the period of 1979/80 to 2017/18. Shadings is DJF Nino3.4 index. Reds (blues) denote El Niño and La Niña events.



Supplementary Figure 8: Same as Fig. S1a, but introducing index of downward longwave radiation (IR) into the monthly CEN.